ELSEVIER

Journal of Alloys and Compounds 306 (2000) 277–284

Journal of ALLOYS AND COMPOUNDS

www.elsevier.com/locate/jallcom

Structural characterization of the aged Inconel 718

C. Slama[a], M. Abdellaoui[b,*]

[a]*E.S.I.E.R, Km 5, Route du Kef, Medjez El Bab, Tunisia*

[b]*National Institute of Research and Physic-Chemistry Analyses, 1 rue Jawhar Sekelli, Menzeh VII, Tunis 1004, Tunisia*

Received 28 December 1999; accepted 22 February 2000

Abstract

The aging of the NC 19 Fe Nb alloy (Inconel 718), previously quenched from 990°C, is characterized by X-ray diffraction, transmission electron microscopy and micro-hardness investigation. The X-ray diffraction patterns reveal the co-existence of the simple cubic, the tetragonal and the orthorhombic structures. These structures correspond respectively to the γ′, γ″ and δ phases. A detailed study of each XRD pattern gives the lattice parameter and the crystalline grain size of the existing phases. TEM observations on thin foils have led to identification of the different phases responsible for the various hardening stages occurring during isothermal tempering performed at 680 and 750°C temperatures for 4, 50 and 100 h. The γ′ and γ″ phase precipitation are strongly dependent on the aging temperature and time. For 680°C aging temperature, hardness investigations show that a first hardening (HV=450) occurs when the duration is about 4 h (the γ′ particle size given by TEM observation is about 5–6 nm). A second hardening (HV=500) was shown to occur at 50 h. It corresponds to the precipitation of the γ″ phase perfectly coherent with the γ matrix. For 750°C aging temperature, the γ″ phase precipitation (coherent with the matrix and the disc shaped with a length of 30 nm) produces a fast hardening after 4 h (HV=466). For a longer thermal exposure, the orthorhombic δ phase appears, reaching a high grain size and fraction volume after 100 h and leading to a drastic microhardness decrease. From 30 nm on, the tetragonal distortion of the γ″ particles increases with increasing precipitate size.

Keywords: Inconel; Superalloy; Hardening; Aging; Precipitation

1. Introduction

Inconel 718 is a nickel-base superalloy largely used in the fabrication of critical pieces for turbine engines because of its high mechanical properties (yield strength up to 650°C, impact strength and fracture toughness down to −40°C), as well as good corrosion resistance. In addition, this alloy can be easily forged and welded. Paulonis et al. [1] showed that the strengthening phase in the alloy 718 is the metastable body centered tetragonal Ni_3Nb (DO_{22}) γ″ phase. This phase is long disc-shaped and lies parallel to the {100} planes of the matrix. The relations between the crystalline structures of the γ″ precipitates and the γ phase are the following:

$$(001)\gamma''\|\{001\}\gamma \quad \text{and} \quad \langle 100\rangle\gamma''\|\langle 100\rangle\gamma.$$

These authors have also shown the existence of a small amount of a γ′ phase $Ni_3(Ti, Al)$ (fcc $L1_2$ structure), appearing as a fine dispersion, of quasi-spherical particles which are coherent with the γ matrix. The role of the γ′ phase is also strengthening, but to a lesser degree than the γ″ precipitates (the volume fraction of γ″ is four times bigger than that of γ′). After treatment at temperatures equal or higher than 750°C, the particle size of the γ″ phase increases rapidly, then these precipitates start to dissolve at the advantage of a stable orthorhombic (DO_a) δ-Ni_3Nb phase: this change induces an overaging of the alloy and some brittleness.

According to Sundararaman et al. [2,3], for an alloy having an (Al+Ti/Nb) ratio equal to 0.66, the strengthening γ′ and γ″ precipitates are formed simultaneously in the 550–660°C temperature range for long time aging. At the opposite, they are simultaneously formed for short time aging in the temperature range of 700 to 900°C. In fact, in the case of alloys presenting a value of this ratio higher than 0.8, Cozar and Pineau [4] have shown that the γ′ phase precipitation precedes the γ″ phase precipitation. The results of Marsh [5] agree with those of Cozar and Pineau [4] in the temperature range of 780 to 820°C.

Moreover, in the case of long duration aging and in the 700–900°C range, we have previously shown the forma-

*Corresponding author. Tel.: +216-1-750-819; fax: +216-1-238-133.

0925-8388/00/$ – see front matter
PII: S0925-8388(00)00789-1

tion of the δ phase [2,3] in addition to those reported above. The δ phase becomes the major one if the treatments are carried out in the 900–1000°C temperature range. Contrary to the γ′ and γ″ phase behaviors, the δ phase seems to have a beneficial effect on stress rupture ductility. The earlier formation of the metastable γ′ and γ″ phases (in comparison to the δ phase) has been attributed to the difference of the lattice mismatches which are weaker in the case of the γ/γ′ or γ/γ″ interfaces than in that of the γ/δ interface.

In this work, we have been mainly interested in the structural investigations of the precipitates resulting from an isothermal aging performed after quenching, as well as in the identification of the phases responsible for the different stages of hardening. On the other hand, by using the X-ray diffraction techniques, we have calculated the values of the lattice parameters and the average grain sizes of the γ″, γ′ and δ phases, respectively.

2. Material and experimental methods

The composition of the Nickel-Base Superalloy 718 is given in Table 1. The alloy was supplied by the 'Acieries Aubert et Duval', as a circular rod having a 68 mm diameter and a 170 mm length. In the as-received state, the heat treatments performed on this rod, after rolling, were as follows: 960°C/1 h/air cooled +720°C/8 h/furnace cooled at 50°C/h to 620°C/8 h/air cooled.

In our study, before every aging test, each specimen was annealed for 30 min at 990°C in a vertical furnace under an argon atmosphere (oxygen content <10 ppm), then water quenched. The aging tests consist of maintaining the sample at two different temperatures — 680°C and 750°C — for three different durations 4, 50 and 100 h followed by water quenching.

The study of the aging, after isothermal tempering, was previously carried out [6,7] with TEM and microhardness techniques:

- Vickers microhardness: the Vickers microhardness tests were performed with a Shimadzu apparatus under a load of 5 N. Each value plotted represents the mean value over 10 measurements.
- TEM examinations: they were carried out using 200 C and 2000 EX JEOL electronic microscopes (the latter operating at 200 kV and equipped with a tilt rotation probe holder). After the aging treatment, the samples were mechanically ground to ~100 μm thickness, then electropolished in a Struers twin-jet unit at 0°C in a bath containing 10 cm^3 perchloric acid, 90 cm^3 ethylic alcohol, under 19 V.
- X-ray diffraction investigation: a small amount of the electrolytically extracted precipitates was glued onto a silica plate for further X-ray diffraction (XRD) investigations. The XRD patterns were obtained using a $(\theta-2\theta)$ Philips diffractometer with Cu Kα radiation ($\lambda=0.15406$ nm). The acquisition conditions were the following ones: $\Delta(2\theta)=0.1°$, Δt/step $(2\theta)=100$ s. A numerical method, the ABFfit program [8], was used to analyze the XRD patterns and to obtain the position and the full-width at half height (FWHH) of the various peaks.

In the ABFfit program [8], the spectrum is modeled by a polynomial background with a maximum degree of two plus a set of simple shaped peaks. The Y value of the pattern is given by the following relation:

$$Y(x) = Bkg(x) + \sum_{i=1}^{n} \text{Peak}_i\,(x, S_i, I_i, X_i, L_i) \quad (1)$$

where 'i' is the index of the 'n' possible peaks, x is the Bragg angle in 2θ, Bkg is a polynomial defining the background, S_i is a peak shape parameter allowing the selection of the appropriate function and I_i, X_i, L_i represent the intensity, position and FWHH of the ith peak.

$$Bkg(x) = b_0 + b_1(x - x_m) + b_2(x - x_m)^2 \quad (2)$$

where x_m is the abscissa of the center of the $[\theta_{\min}, \theta_{\max}]$ angular region of the observed pattern.

The functions which describe the peaks have been reparameterized in the ABFfit program as a function of the integrated intensity 'I', the mean position of the peak 'x_m' and the FWHH 'L', and are of three kinds: Gaussian, modified Lorentz or Cauchy. Such a method has been previously applied by Abdellaoui [9], Gaffet and Harmelin [10] and Cocco et al. [11].

The effective crystalline grain size (hereafter referred to

Table 1
Chemical composition of the INCONEL 718 alloy

wt.%	Ni	Fe	Cr	Nb+Ta	Mo	Ti	Al	Co	Si
	52.94	19.22	17.94	5.11	2.95	0.93	0.53	0.14	0.04
wt.%	Mn	Cu	Ca	Mg	Pb	C	B	S	P
	0.04	<0.10	<0.002	<0.003	<0.001	0.034	<0.005	<0.002	0.009
at.%	Ni	Fe	Cr	Nb	Mo	Ti	Al	Ti+Al/Nb	Ti/Al
	52.58	20.06	20.10	3.20	1.79	1.13	1.14	0.71	0.99

as Φ (Å)) have been calculated from Scherrer's expression:

$$\Phi = \frac{0.9\lambda}{L\cos(\theta)} \quad (3)$$

where L and θ are, respectively, the FWHH and the angular peak position (in 2θ) of the Gaussian contribution of the crystalline peak. The Bragg expression was applied to determine the inter-reticular distance value corresponding to the diffraction peak position θ:

$$\lambda = 2d\sin(\theta). \quad (4)$$

The precipitates used in the XRD investigations were electrolytically extracted from the heat treated specimens. The solution used for the extraction of precipitates consisted of 10 vol.% of HCl in methanol (V=220 mV, extraction time=5 to 6 h).

3. Experimental results and discussion

Different specimens were submitted to isothermal tempering at two different temperatures, 680°C and 750°C: these two temperatures were determined from the dilatometric behavior of a specimen in the quenched state submitted to a continuous heating [12].

3.1. Micro-hardness investigation

Fig. 1a shows the hardness change as a function of the tempering duration at different temperatures. At 680°C, the temperature is sufficiently high to allow the diffusion to be operative and to induce a rapid strengthening; consequently, the volume fraction of precipitates will be more important and the maximum value will be the highest (HV=500). Furthermore, it will be underlined, that the hardening takes place in two successive steps (the second starting only after 20 h of tempering).

At 750°C, the diffusion rate is still higher and the hardening kinetics is faster, in such a way that after a 4-h tempering, the hardness is equal to 465. However, the coarsening of precipitates leads rapidly to a hardness decrease. In fact, the higher the duration of the isothermal soaking the lower is the hardness value.

3.2. TEM microstructural investigation of precipitates

3.2.1. Microhardness evolution versus precipitate grain size

Transmission electron microscopy (TEM) examinations were made on thin foils heat treated at 680 and 750°C in states for which the hardness presents particular values.

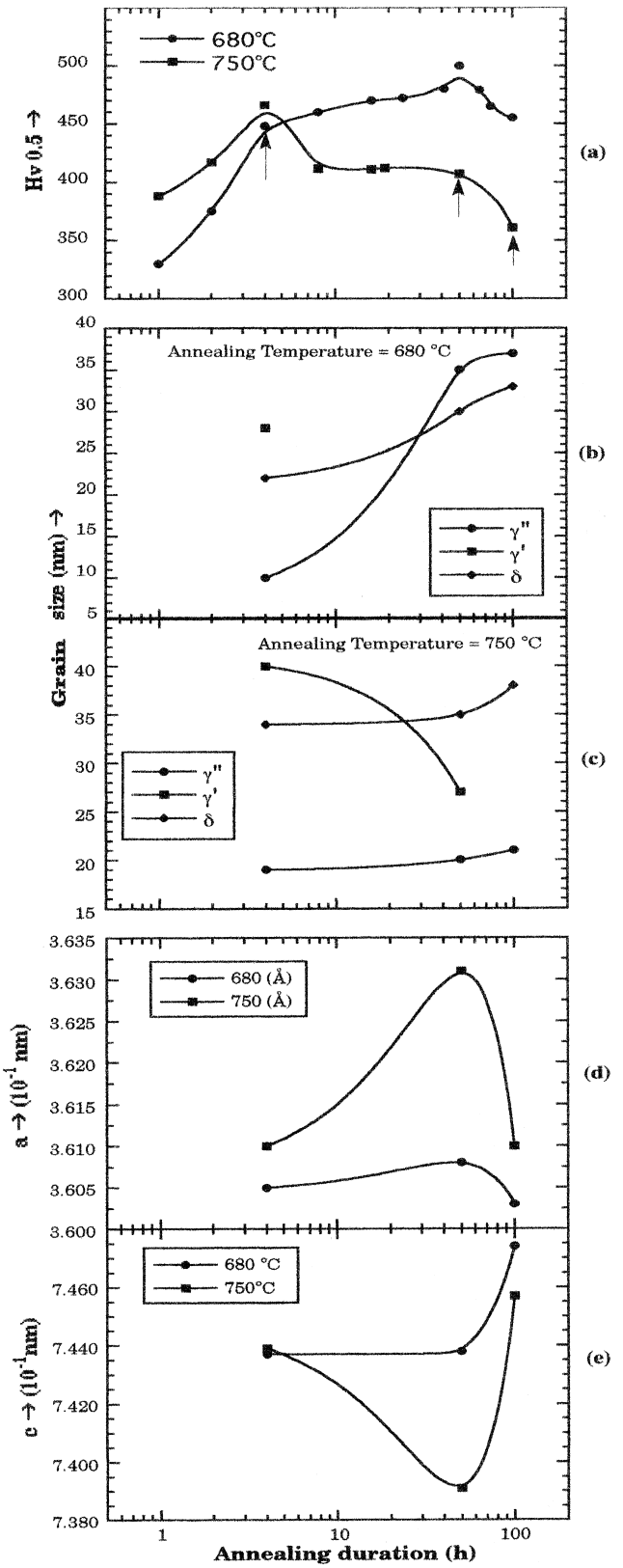

Fig. 1. (a) Microhardness variation as a function of the aging duration for 680 and 750°C. γ', γ'' and δ grain size variation as a function of the annealing duration at (b) 680 and (c) 750°C. Variation of (d) the γ'' lattice parameter 'a' and (e) the γ'' lattice parameter 'c' as a function of the annealing duration for 680 and 750°C.

3.2.1.1. Aging at 680°C

After a 4-h treatment at 680°C, the dark-field micrograph (obtained using the (110) super lattice reflection) shows an important precipitation of very fine and evenly distributed particles (Fig. 2) which are not clearly discernible.

However, the finer precipitates are spherical suggesting the predominance of the γ′ phase. This is in agreement with the XRD patterns corresponding to the sample aged for 4 h which exhibits the {111}, {211} and {220} lines, characteristic of the γ′ phase (Fig. 6a). So, the increase of hardness (HV=450) suggests that the γ′ phase is responsible for the material hardening as was previously concluded [6].

As previously reported [6], the visibility of the precipitates is enhanced considerably when increasing the aging time (50 h). In dark-field obtained from $(\bar{1}10)$ γ″ spot, these latter appear as long disc-shaped, uniformly distributed in the matrix with a very high number density. Moreover, we can easily see that at the tip of these γ″ precipitates, some small γ′ spherical particles may be observed. So, we can conclude that this $(\bar{1}10)$ superlattice reflection belongs to the γ′ and γ″ precipitates. Paulonis et al. [1] show that the {100} and {110} reflections could arise both from γ′ and γ″ precipitates. The mean length of the γ″ disc precipitates is about 30 nm. This latter is assumed to be responsible for the strengthening in this case. However, controversies still exist concerning the formation sequence of the γ″ and γ′ phases [4,6,13,14].

We have previously reported [6] that after 100 h of aging, some δ platelet phases are formed at the grain boundaries which are 0.26 μm in size and are parallel between them in one of the grains. The growing of these δ lamellar precipitates in this grain creates a γ″ free zone in the interlamellar spaces and all along the grain boundary. This free zone has been previously observed by several authors [2,15–17] who have shown that such a γ′ free zone is an indication of the Nb depletion adjacent to the delta precipitates. The γ″ precipitates are ~50 nm in length. So, the hardness decrease will be attributed to the δ phase particle coarsening and its volume fraction increase.

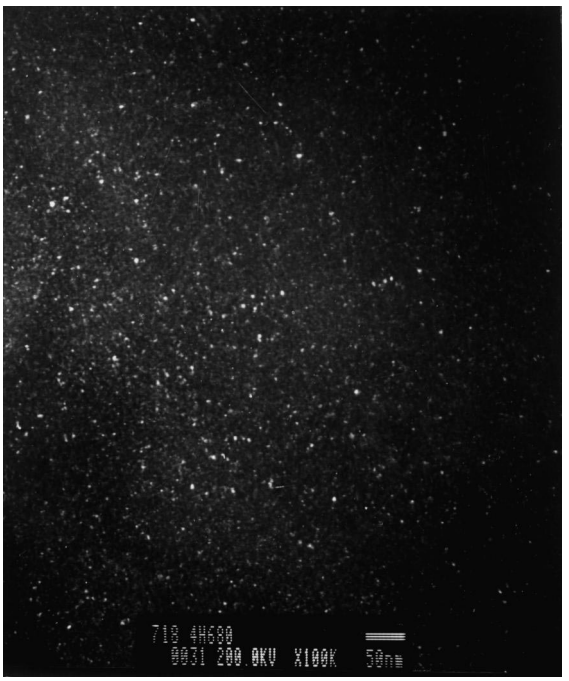

Fig. 2. Dark-field micrograph, corresponding to the sample treated for 4 h at 680°C, obtained using the (110) super lattice reflection.

3.2.1.2. Aging at 750°C

It has been reported [6] that the TEM observations show a very abundant precipitation of the γ″ particles which are homogeneously distributed in the matrix after 4 h aging. These γ″ precipitates are lens-shaped having an average length about 30 nm. Moreover, it will be noted the presence of spherical shaped γ′ particles, usually pinned on the γ″ plates. The precipitation of the δ platelets takes place at the γ grain boundary whereas their growth is shown to occur inside the γ grain at the expense of the γ″ precipitates [6]. More attention has to be paid to the high abundance of the γ″ phase, as compared to the other phases present at this aging treatment. So, we assume that the high microhardness value (HV=465) (Fig. 1a) is induced by the high γ″ proportion in the material.

For a tempering duration of 50 h, the γ″ precipitates change in shape during coarsening. The average length of these particles is 80 nm. Yet, it is necessary to note the presence of the γ′ precipitates which are distinct or associated to γ″ particles [6]. Similarly, we note the growth of the δ platelets. So, we assume that the decrease in hardness value (Fig. 1a) will be attributed to the γ″ particles coarsening.

When increasing the aging duration up to 100 h, γ″ precipitates look like thin platelets, while γ′ particles have spherical shapes (Fig. 3). Similarly, the volume fraction of the γ″ precipitates decreases contrarily to its grain size. The mean length of them is about 120 nm.

Often, the δ precipitates form at the expense of the γ″ ones which are progressively dissolved. So, only a few γ′ spherical precipitates remain between δ platelets and a γ″ denuded zone adjacent to the γ boundary appears (Fig. 4). This zone is about 0.4 μm in width. Similar results have been observed by Burke and Miller [17]. The volume fraction of δ phase increases with increasing the aging temperature and time. Indeed, during a tempering at 750°C for 100 h, δ precipitation occurred at intragranular sites. According to Sundararaman et al. [3], the intragranular nucleation mode of the δ phase is related to the staking faults within the γ″ precipitates. So, it can be easily concluded that the drastic decrease in the microhardness value is first due to the fast coarsening and partial dissolution of the γ″ phase and second to the δ phase volume fraction increase. Table 2 gives mean grain size of

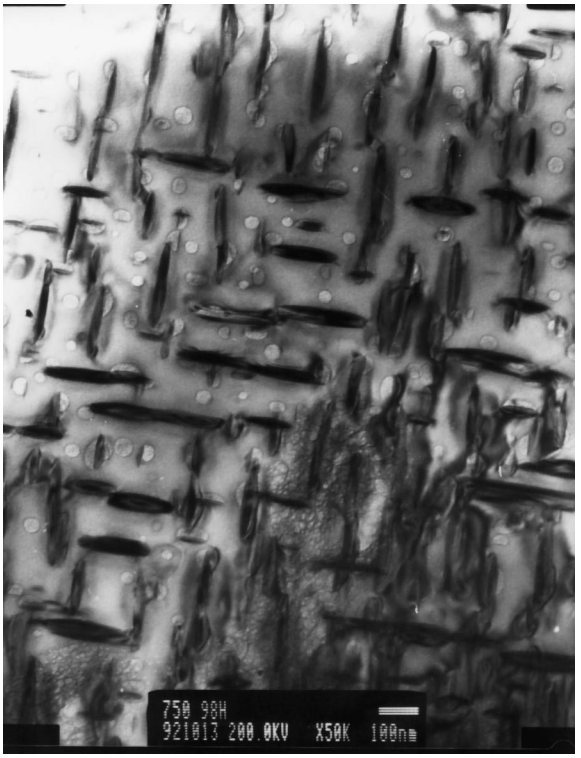

Fig. 3. Precipitation of the γ″ and γ′ phases at 750°C for 100 h (bright field).

Fig. 4. A bright field micrograph showing the growing of the δ particles and the presence of the γ″ denuded zone near the precipitates obtained at 750°C for 100 h.

Table 2
Mean grain size values of the γ′ and γ″ phases calculated from TEM observations. The parameters L, e and ϕ mean, respectively, the length, the thickness and the diameter of the grains

Phase	Aging temperature (°C)	Aging time (h) 4	50	100
γ″	680	$L=10$ nm	$L=30$–35 nm $e=11$ nm	$L=50$ nm $e=13$ nm
	750	$L=30$ nm $e=9$ nm	$L=80$–90 nm $e=17$ nm	$L=120$ nm $e=22$ nm
γ′	680	$\phi=6$ nm	$\phi=12$ nm	$\phi=16$ nm
	750	$\phi=8$ nm	$\phi=26$ nm	$\phi=33$ nm

γ′ and γ″ phases for the different aging conditions determined by TEM observations.

3.2.2. Tetragonal distortion

The relationship between the constrained strain, ε^c, and the stress-free strain, ε^T, for an ellipsoidal precipitate exhibiting a tetragonal distortion perpendicular to its habit plane is given by [18]:

$$\varepsilon^c = \left[1 - \frac{(1-2\upsilon)}{2(1-\upsilon)}\frac{a}{R}\right]\varepsilon^T$$

where $a = 4h/3$ is the thickness of the ellipsoidal particle with major axis R and minor axis h and υ is the Poisson's ratio ($\upsilon = 1/3$ and $\varepsilon^T = 0.0286$).

Fig. 5 gives the variation of the constrained strain, ε^c, versus the precipitate size obtained for the different aging conditions. Based on this figure, we can see that for an aging at 750°C, the tetragonal distortion increases when increasing the particle size and the aging duration from 0.0257 for 30 nm (4 h) to about 0.0268 for 120 nm particle size (100 h). However, for an aging at 680°C, this tetragonal distortion decreases from about 0.0257 for 10

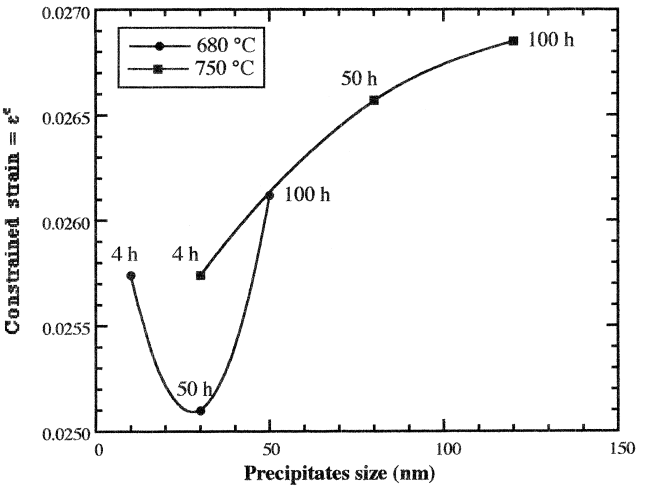

Fig. 5. Variation of the constrained strain, ε^c, versus the precipitate size obtained for the different aging conditions.

nm (4 h) to about 0.0251 for 30 nm (50 h) and then increases to reach 0.0261 for 50 nm particle size (100 h).

On the other hand, when the γ″ particle size exceeds 30 nm, the tetragonal distortion increases and the microhardness decreases when increasing the particle size. So, we assume that the microhardness value is more affected by the particle coarsening and the type of the strengthening phase than by the tetragonal distortion. This latter will normally lead to microhardness increase as a result of a strain hardening.

3.3. XRD structural investigation of precipitates

The X-ray diffraction patterns show the existence of the following phases: the γ′ and/or the γ″ strengthening phases, the Nb–Ti rich phase, the TiN phase, an MC type carbide and Ni_3Nb type δ phase. The last two phases are detected in all specimens. The identification of the Nb–Ti rich phase is done according to Hajmrle et al. [19]. Concerning the chemical composition of the MC type carbide, energy dispersive X-ray microanalyses results, reported earlier [7], suggested that the M atom was a (Nb, Ti) combination.

Fig. 6 gives the XRD patterns of the various aging conditions. The deconvolution of each of them using the ABFfit program, explained above, leads to the determination of the various phases, listed above, existing in the material as well as the corresponding lattice parameters and crystalline grain size. The values of these parameters are summarized in Table 3.

3.3.1. Variation of grain size versus heat treatment

In XRD investigations, the deconvolution of the pattern leads to the determination of the spherical coherent domain size. In the case of non-agglomerated particles, the coherent domain size corresponds to the particle size or also to the grain size determined by TEM. On the contrary, when the particles agglomerate, the coherent domain size is equal to the individual particle size and the grain size will be the sum of these individual particle sizes. Consequently, the grain size contribution determined by XRD will be different from that determined by TEM.

On the other hand, when the grains are not spherical, XRD investigation gives a mean value of the grain dimensions. So, in the case of shape texture, the XRD contribution will give the dimension perpendicular to the texture axis. So, in the γ″ case, XRD investigation will give the thickness, the length or a mean value of them as a crystalline grain size.

Fig. 1b and c gives the variation of the grain size of the γ′, γ″ and δ phases as function of the annealing duration, respectively, at 680 and 750°C. In the case of the 680°C treatment, it has to be noticed that for 4 h duration the γ′ grain size is more important than those of γ″ and δ. This result supports what has been concluded by TEM observation concerning the responsibility of γ′ for the hardening

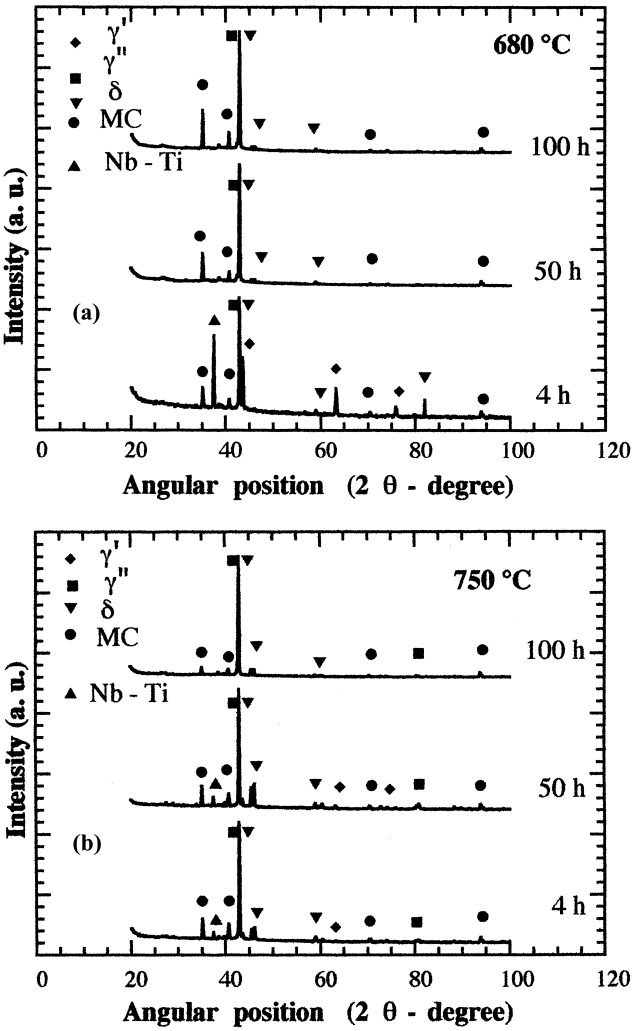

Fig. 6. X-ray diffraction patterns corresponding to samples annealed for different duration at (a) 680°C and (b) 750°C.

in this case. When increasing the aging time until 50 h, the XRD patterns do not show the γ′ lines and the γ″ becomes the dominant phase. Its grain size reaches 35 nm. So, the microhardness value will be greatly affected by the γ″ phase. This is in agreement with our TEM observation conclusions. For longer duration (100 h), we note a simultaneous increase of the γ″ and δ phases grain size with a decrease of the γ″ volume fraction. This behavior leads to a microhardness decrease, because of the poor hardening behavior of the δ phase.

For 750°C aging, the deconvolution of the XRD patterns seems to give not the length of the γ″ particles but their thickness. For 4 h aging, the γ′ grain size value is the highest, but the γ″ is abundant. So, the maximum value reached by the microhardness (HV=466) will be induced more by the γ″ hardening than that of the γ′ one. As the aging time increases, the γ″ and the δ particles coarsen more and more with volume fraction abundance of the δ phase which consummate the Nb at the expense of the γ″ phase. So, we assume that the drastic decrease of the

Table 3
Lattice parameters (a, b, c) and grain size (ϕ) mean values of the γ″, γ′ and δ phases calculated from XRD patterns

Phase	Aging temperature (°C)	Aging time (h)		
		4	50	100
γ″	680	a=0.3605 nm	a=0.3608 nm	a=0.3603 nm
Body-centered		c=0.7437 nm	c=0.7438 nm	c=0.7474 nm
tetragonal (bct)		c/a=2.0629	c/a=2.0615	c/a=2.0743
		ϕ=10 nm	ϕ=35 nm	ϕ=37 nm
	750	a=0.3610 nm	a=0.3631 nm	a=0.3610 nm
		c=0.7439 nm	c=0.7391 nm	c=0.7457 nm
		c/a=2.0606	c/a=2.0355	c/a=2.0656
		ϕ=19 nm	ϕ=20 nm	ϕ=21 nm
δ	680	a=0.5105 nm	a=0.5108 nm	a=0.5110 nm
Orthorhombic		b=0.4209 nm	b=0.4220 nm	b=0.4216 nm
		c=0.4529 nm	c=0.4521 nm	c=0.4526 nm
		ϕ=22 nm	ϕ=30 nm	ϕ=33 nm
	750	a=0.5111 nm	a=0.5106 nm	a=0.5108 nm
		b=0.4214 nm	b=0.4225 nm	b=0.4218 nm
		c=0.4531 nm	c=0.4557 nm	c=0.4530 nm
		ϕ=34 nm	ϕ=35 nm	ϕ=38 nm
γ′	680	a=0.3592 nm	–	–
Face centered cubic		ϕ=28 nm		
(fcc)	750	a=3593 nm	a=3596 nm	–
		ϕ=40 nm	ϕ=27 nm	

microhardness value in the 50–100 h time range is induced by the precipitation of the δ phase and the dissolution of the γ″ one. This statement is in agreement with our TEM observation. The γ′ strengthening phase was detected only for an aging for 4 h at 680°C or an aging for 4 and 50 h at 750°C. This is shown by the single square point in Fig. 1b and the two square point in Fig. 1c.

3.3.2. Variation of γ″ lattice parameters versus heat treatment

Fig. 1d and e show, respectively, the variation of the γ″ lattice parameters a and c calculated from XRD patterns for samples aged at 680 and 750°C. Based on Fig. 1d and e, we can see that for 680°C aging, the lattice parameters a and c increase slightly when increasing the aging duration from 4 up to 50 h to reach, respectively, 0.3608 and 0.7438 nm. These lattice parameters were, respectively, equal to 0.3605 and 0.7437 nm at an aging duration of 4 h. For aging duration greater than 50 h, the c lattice parameter increases drastically to reach a value of 0.7474 nm for 100 h aging duration. Whereas, the a lattice parameter slightly decreases to reach 0.3603 nm for 100 h maintaining duration. In other words, the γ″ lattice undergoes an isotropic expansion along the two axes $\vec{a}$ and $\vec{c}$ until 50 h duration. For longer duration, the γ″ lattice undergoes an expansion along the $\vec{c}$ axis and a compression along the $\vec{a}$ axis. The c/a ratio remains unchanged and equal to 2.062–2.063 when increasing the duration from 4 up to 50 h and then increases to reach 2.074 for 100 h. The c/a increase will induce more distortion of the γ″ lattice and then more increase of the microhardness value. However, for 4 h aging, the sample is γ′ rich material and its hardness will depend only on the strengthening degree of this phase. This latter phase is a strengthening phase but at a lesser degree than the γ″ one. At 50 h duration, the sample is a γ″ rich material and its hardness will only depend on the γ″ strengthening degree. We assume that, as the c/a ratio remains unchanged, there was no effect of lattice distortion and the hardness is only affected by the γ″ strengthening phase. So, it increases to reach 500 HV. For longer times, the sample is a δ-softening-phase-rich material. So, we will have a decrease of the hardness even if the c/a ratio, and consequently the lattice distortion, increase.

Based on Fig. 1d and e, we can see that for 750°C aging, the lattice parameters a and c vary in opposite directions: the 'a' lattice parameter increases progressively from 0.3610 nm to 0.3631 nm when increasing the aging duration from 4 up to 50 h, whereas the 'c' lattice parameter decreases at the same rate from 0.7439 nm to 0.7391 nm when the maintaining duration increases from 4 to 50 h. For aging duration greater than 50 h, the lattice parameters a and c vary in the opposite direction but in a way opposite to the latter one. In fact, the 'a' lattice parameter decreases progressively from 0.3631 nm to 0.3610 nm when increasing the aging duration from 50 up to 100 h, whereas the 'c' lattice parameter increases at the same rate from 0.7391 nm to 0.7457 nm when the maintaining duration increases from 50 to 100 h. In other words, the γ″ lattice undergoes an expansion along the $\vec{a}$ and a compression along the $\vec{c}$ axes until 50 h of maintaining. For higher maintaining duration, the compression and expansion phenomena go in an opposite way to the latter one.

Based on TEM observations, the strengthening phase for

the 4 and 50 h maintaining duration is the γ″ precipitate with coarsened grains for 50 h. For 100 h maintaining, the δ phase is predominant. On the other hand, the c/a ratio decreases from 2.061 to 2.04 when the aging increases from 4 to 50 h. This c/a decrease will induce the decrease of the γ″ lattice distortion. So, we assume that the grain size coarsening and lattice distortion decrease are mainly responsible for the microhardness decrease. For aging time higher than 50 h, the c/a ratio and then the γ″ lattice distortion increases to reach 2.066 for 100 h. However, for 100 h aging time, as the δ precipitate is the predominant phase, the γ″ lattice distortion has no effect.

4. Conclusion

Based on the results described above, the following conclusions can be drawn.

1. At 680°C, γ′ precipitation appears to precede γ″ precipitation. Indeed, a first hardening occurs at 4 h aging which has been related to spherical-shaped γ′ precipitates as confirmed by X-ray diffraction experiments. Beyond this duration, the sample is a γ″ rich material and even if the γ″ lattice parameters undergo an isotopic expansion along the two axes $\vec{a}$ and $\vec{c}$, the c/a ratio remains unchanged. So, there was no effect of lattice distortion and the hardness (500 HV) is only affected by the γ″ strengthening degree. When the aging duration exceeds 50 h (30 nm in grain size), the γ″ lattice undergoes an expansion along the $\vec{c}$ axis and a compression along the $\vec{a}$ axis which induces the increase of the c/a ratio. However, contrarily to what will be obtained as an effect of the lattice distortion increase, we see a decrease in the hardness value for the 680°C/100 h treatment. This will be due to the δ brittle phase effect.
2. At 750°C, high abundance and coarsening of the γ″ precipitates (30 nm in length) produce a fast hardening even after a 4-h treatment (HV=466). For 50 h aging time, the microhardness decrease will be probably due to a considerable coarsening of the γ″ precipitates (80 nm) and the c/a ratio decrease. Contrarily, beyond this aging duration, the hardness is not affected by the lattice distortion and the decrease in hardness for 100 h treatment is due to the rapid coarsening of the γ″ precipitates (120 nm) and the volume fraction increase of the δ phase.
3. Even at 680 or 750°C aging temperature, the tetragonal distortion and the microhardness values of the γ″ precipitates vary in opposite ways. However, it will be noted that when the γ″ particle size exceeds 30 nm, the tetragonal distortion increases with increasing precipitate size.

References

[1] D.F. Paulonis, J.M. Oblak, D.S. Duvall, Trans. ASM 62 (1969) 611–622.
[2] M. Sundararaman, P. Mukhopadhyay, S. Banerjee, Met. Trans. 19A (3) (1988) 453–465.
[3] M. Sundararaman, P. Mukhopadhyay, S. Banerjee, in: E.A. Loria (Ed.), Super Alloys 718, 625, 706 and Various Derivatives, The Minerals, Metals and Materials Society, Warrendale, PA, 1994, pp. 419–440.
[4] R. Cozar, A. Pineau, Metall. Trans. 4 (1973) 47–59.
[5] A.E. Marsh, Metallurgia (1982) 10–20.
[6] C. Slama, C. Servant, G. Cizeron, J. Mater. Res. 12 (9) (1997) 2298–2316.
[7] C. Slama, G. Cizeron, J. Phys. III 7 (1997) 665–688.
[8] A. Antoniadis, J. Berruyer, A. Filhol, International Report 87AN22T, Institute Lauë Langevin, Grenoble, 1988.
[9] M. Abdellaoui, J. Alloys Comp. 264 (1998) 285–292.
[10] E. Gaffet, M. Harmelin, J. Less-Common Metals 157 (1990) 201.
[11] G. Cocco, S. Enzo, S. Schiffini, L. Battezzati, Mater. Sci. Eng. 97 (1988) 43.
[12] C. Slama, Thèse de Doctorat en Science, Université de Paris-Sud, Centre d'Orsay, 1993.
[13] A.O. Basile, J.F. Radavich, in: Superalloys 718, 625 and Various Derivatives, The Minerals, Metals and Materials Society, Warrendale, PA, 1991, pp. 325–335.
[14] J.L. Burger, R.R. Biederman, W.H. Courts, in: Superalloy 718 — Metallurgy and Applications, The Minerals, Metals and Materials Society, Warrendale, PA, 1989, pp. 207–217.
[15] I. Kirman, J. Iron Steel Inst. 207 (1969) 1612–1618.
[16] R. Cozar, Thèse de Docteur-Ingénieur, Université de Nancy 1, 1973.
[17] M.G. Burke, M.K. Miller, in: Superalloys 718, 625 and Various Derivatives, The Minerals, Metals and Materials Society, Warrendale, PA, 1991, pp. 337–350.
[18] M. Sundararaman, P. Mukhopadhyay, S. Banerjee, Metall. Trans. 23A (1992) 2015–2028.
[19] K. Hajmrle, R. Angers, G. Dufour, Metall. Trans. 13A (1982) 5–12.